Blind Source Separation and Deconvolution of Dynamic Medical Image Sequences

Ondřej Tichý[1,2]

[1] Institute of Information Theory and Automation
[2] Faculty of Nuclear Sciences and Physical Engineering

Seminář strojového učení a modelování
21.11.2013

Supervisor: Václav Šmídl (UTIA)

Outline

- ▶ Problem description
- ▶ Current approaches
- ▶ Blind source separation (BSS)
- ▶ Deconvolution in BSS (BCMS)
- ▶ Automatic regions of interest in BSS (FAROI)
- ▶ Automatic relevant determination and deconvolution in BSS (S-BSS-vecDC)
- ▶ On validation of the algorithms
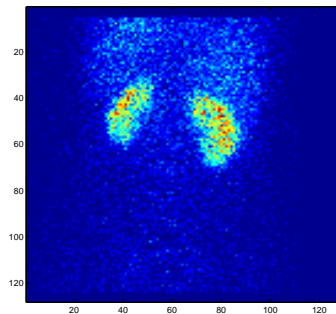
Problem description

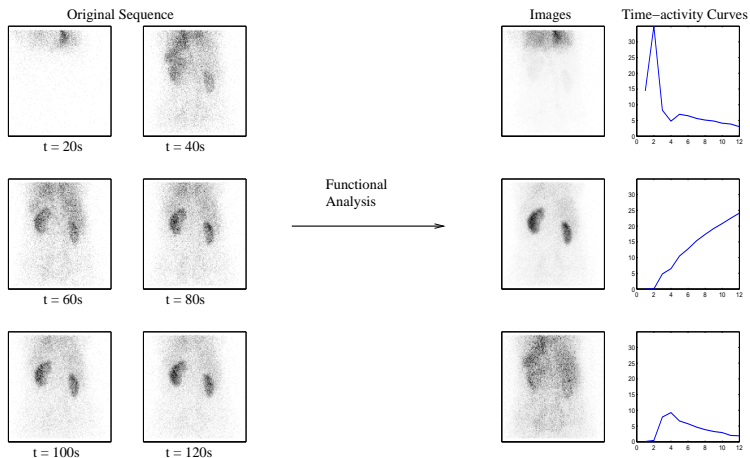The scheme of scintigraphy:
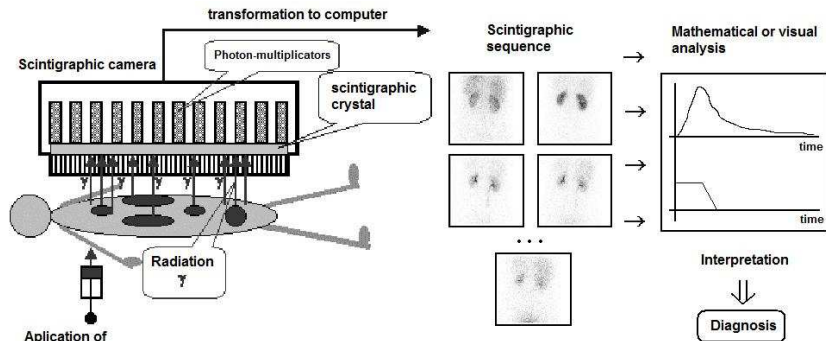
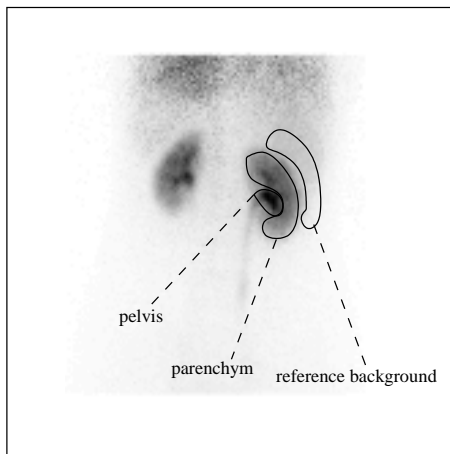# Problem description

CT:

Scintigraphy:

Problem description

The scheme of tissues detection from renal scintigraphy sequence:

Original Sequence

t = 20s   t = 40s

t = 60s   t = 80s

t = 100s   t = 120s

Functional Analysis

Images   Time−activity Curves

Problem description

pelvis

parenchym

reference background

Problem description

Why should we do that?

Problem description

Why should we do that?
e.g. Relative Renal Function (RRF) computation in clinical practise:

- Computed from parenchyma activity during accumulation.
- L_p is activity in the left parenchyma.
- R_p is activity in the right parenchyma.
- RRF (for the left kidney):

$$\text{RRF} = \frac{L_p}{L_p + R_p} \tag{1}$$

Current Approaches

▶ It is possible to select a specific region and obtain its
  activity in time.
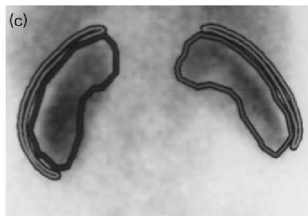
[M. Caglar et al., Nuclear medicine communications, vol. 29, no. 11, p. 1002, 2008.]

Current Approaches

- It is possible to select a specific region and obtain its activity in time.

(c)

[M. Caglar et al., Nuclear medicine communications, vol. 29, no. 11, p. 1002, 2008.]

- Clear activity of parenchyma can be achieved by subtraction of reference background.
- Problems: it is very time consuming and highly dependent on physician.
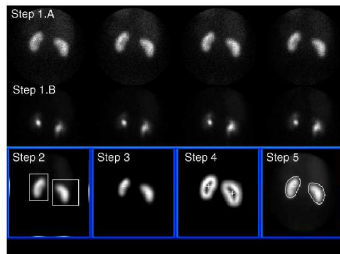
Current Approaches

Kidneys borders can be found using software AUTOROI.
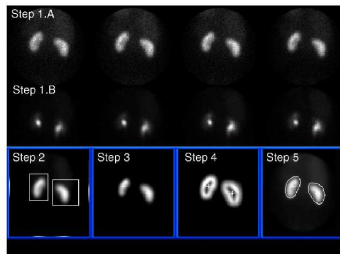
[E. Garcia et al., Nuclear medicine communications, vol. 31, no. 5, p. 366, 2010.]

Current Approaches

Kidneys borders can be found using software AUTOROI.

[E. Garcia et al., Nuclear medicine communications, vol. 31, no. 5, p. 366, 2010.]

- ▶ Focused only on kidney border.
- ▶ Manual interaction is necessary.

Current Approaches

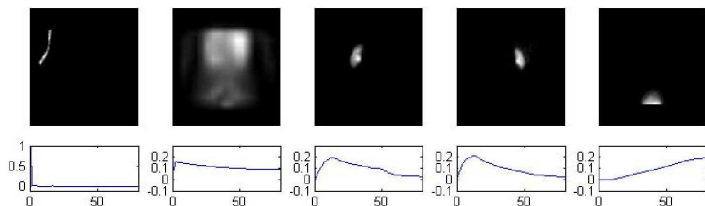Dynamic renal study is examined in [Ståhl et al. 2011]; based on compartment modeling.

Fig. 6. The injection, blood/tissue, left kidney, right kidney and bladder compartments

[D. Ståhl et al., Image Analysis, 557-568, Springer Berlin Heidelberg, 2011.]

Current Approaches

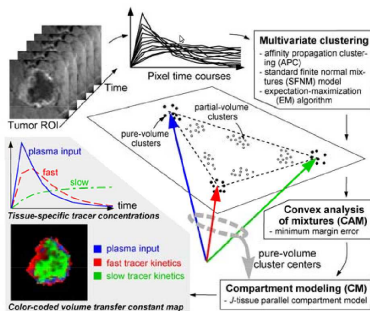Dynamic renal study is examined in [Ståhl et al. 2011]; based on compartment modeling.
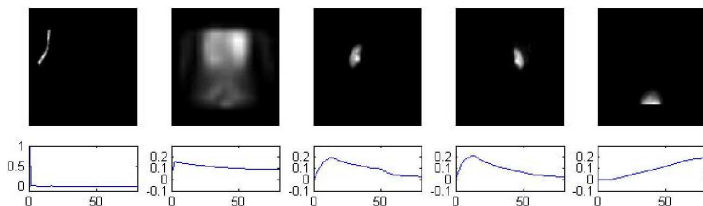
Fig. 6. The injection, blood/tissue, left kidney, right kidney and bladder compartment

[D. Ståhl et al., Image Analysis, 557-568, Springer Berlin Heidelberg, 2011.]

- ▶ A whole kidney is one compartment.
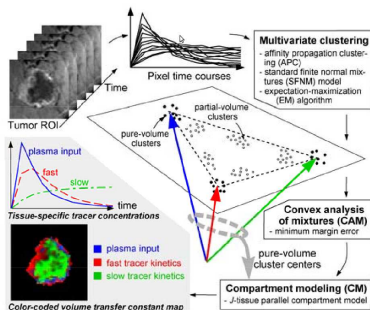
Current Approaches

Dynamic studies of tumor are examined in [Chen et al. 2011].

[L. Chen et al., Medical Imaging, IEEE Transactions on, no. 99, pp. 1-16, 2011.]

Current Approaches

Dynamic studies of tumor are examined in [Chen et al. 2011].

[L. Chen et al., Medical Imaging, IEEE Transactions on, no. 99, pp. 1-16, 2011.]

- ▶ Manual setting of number of compartments is necessary.
- ▶ Huge computation issues.

Scalar Example of Blind Source Separation

► Consider following scalar model:

$$d = ax + e \qquad (2)$$

Scalar Example of Blind Source Separation

- Consider following scalar model:

$$d = ax + e \tag{2}$$

- Since $e \sim \mathcal{N}(0, r_e)$, then

$$f(d|a, x, r_e) = \mathcal{N}(ax, r_e) \tag{3}$$

and priors for a and x are chosen as

$$f(a|r_a) = \mathcal{N}(0, r_a) \tag{4}$$
$$f(x|r_x) = \mathcal{N}(0, r_x) \tag{5}$$

Scalar Example of Blind Source Separation

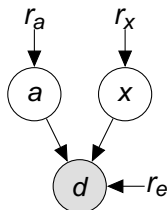- Consider following scalar model:

$$d = ax + e \qquad (2)$$

- Since $e \sim \mathcal{N}(0, r_e)$, then

$$f(d|a, x, r_e) = \mathcal{N}(ax, r_e) \qquad (3)$$

and priors for a and x are chosen as

$$f(a|r_a) = \mathcal{N}(0, r_a) \qquad (4)$$

$$f(x|r_x) = \mathcal{N}(0, r_x) \qquad (5)$$

Scalar Example of Blind Source Separation

- ▶ Following Variational Bayes (VB) method, we construct the posterior density and compute estimates of parameters a and x using iterative algorithm.
- ▶ Iterative VB algorithm estimates parameter using estimates of others.

Scalar Example of Blind Source Separation

- ▶ Following Variational Bayes (VB) method, we construct the posterior density and compute estimates of parameters *a* and *x* using iterative algorithm.
- ▶ Iterative VB algorithm estimates parameter using estimates of others.
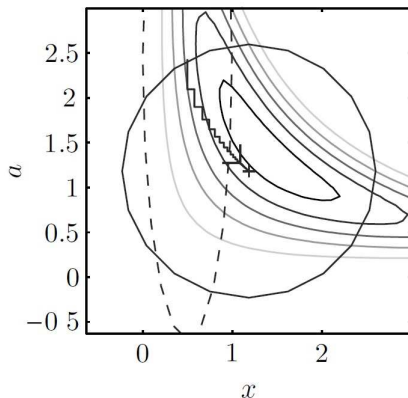
Blind source separation (BSS)

- Each recorded image is a superposition of biological tissues:

$$\mathbf{d}_t = \mathbf{a}_1 x_{1,t} + \mathbf{a}_2 x_{2,t} + \cdots + \mathbf{a}_r x_{r,t} \tag{6}$$

- t is the time index
- r is the number of physiological tissues
- $\mathbf{d}$ is the observed image (stored column-wise)
- $\mathbf{a}_k$ is the image of the kth tissue (stored column-wise)
- $x_{k,t}$ is the weight of the kth tissue image in time t

Blind source separation (BSS)

[J.W. Miskin. Ensemble learning for independent component analysis, PhD thesis, University of Cambridge, 2000.]

Problem specifics:

- ▶ Poisson observation noise.
- ▶ Positivity of tissue images and time-activity curves.
- ▶ Unknown number of tissues.

Blind source separation (BSS)

Problem specifics:

- Poisson observation noise.
- Positivity of tissue images and time-activity curves.
- Unknown number of tissues.

$$f(\mathbf{d}_t | A, X, \omega) = \text{t}\mathcal{N}(A\bar{\mathbf{x}}_t, \omega^{-1} I_p \otimes I_n), \qquad (7)$$
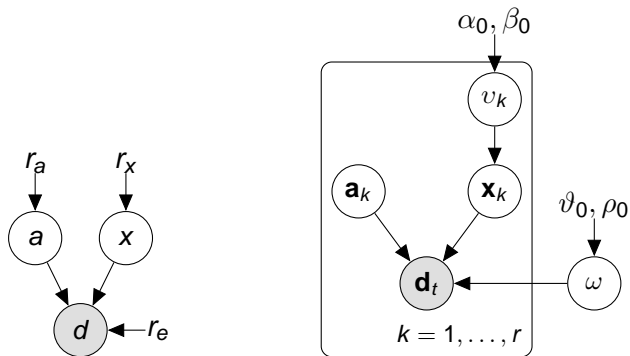
$$f(\omega) = \text{G}(\vartheta_0, \rho_0), \qquad (8)$$

$$f(\mathbf{x}_k | \upsilon_k) = \text{t}\mathcal{N}(0_{n,1}, \upsilon_k^{-1} I_n), \qquad (9)$$
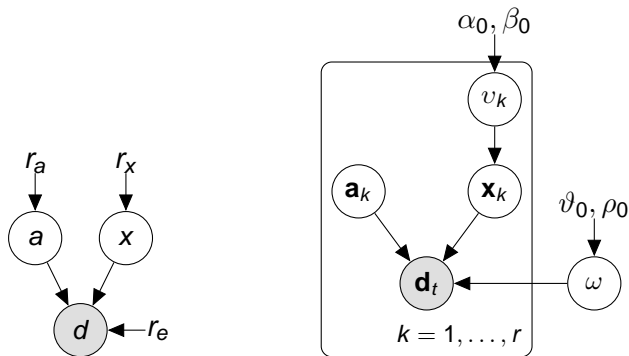
$$f([\upsilon_1, \ldots, \upsilon_r]) = \prod_{k=1}^{r} \text{G}(\alpha_{k,0}, \beta_{k,0}), \qquad (10)$$

$$f(\mathbf{a}_k) = \text{t}\mathcal{N}(0_{p,1}, I_p), \qquad (11)$$

Ondřej Tichý   Blind Source Separation and Deconvolution of Dynamic Medical Image Sequences

Blind source separation (BSS)

Blind source separation (BSS)

- Note that biologically meaningful solution is not guaranteed.

Deconvolution in BSS (BCMS)

[O. Tichý, V. Šmídl, and M. Šámal. In ECCOMAS Conf. on Comp. Vision and Medical Image Proc., 2013.]

Motivation:

- ▶ The time-activity curves of tissues are convolution of the input activity (the blood) and tissue-specific kernels.

Deconvolution in BSS (BCMS)

[O. Tichý, V. Šmídl, and M. Šámal. In ECCOMAS Conf. on Comp. Vision and Medical Image Proc., 2013.]

Motivation:

- ▶ The time-activity curves of tissues are convolution of the input activity (the blood) and tissue-specific kernels.
- ▶ The shape of the kernels is expected to be formed by a constant plateau followed by monotonic decrease to zero.
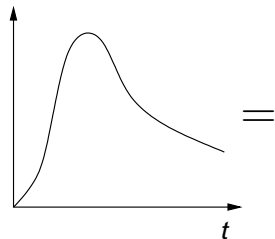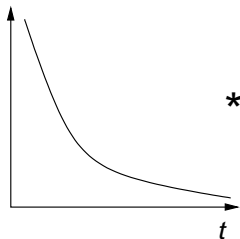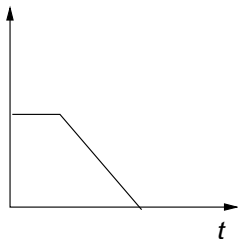
Deconvolution in BSS (BCMS)

[O. Tichý, V. Šmídl, and M. Šámal. In ECCOMAS Conf. on Comp. Vision and Medical Image Proc., 2013.]

Motivation:

- The time-activity curves of tissues are convolution of the input activity (the blood) and tissue-specific kernels.
- The shape of the kernels is expected to be formed by a constant plateau followed by monotonic decrease to zero.

Organ time activity, x_f Blood time activity, b Convolution kernel u_f

=   *

t t t

Deconvolution in BSS (BCMS)

- Each time-activity curve, $\mathbf{x}_k$, is modeled as a convolution:

$$x_{t,k} = \sum_{m=1}^{t} b_{t-m+1} u_{m,k} \qquad (12)$$
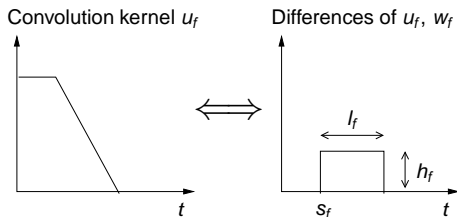
Deconvolution in BSS (BCMS)

- Each time-activity curve, $\mathbf{x}_k$, is modeled as a convolution:

$$x_{t,k} = \sum_{m=1}^{t} b_{t-m+1} u_{m,k} \tag{12}$$

- Convolution kernels of each tissue are modeled as additions stored in vectors $\mathbf{w}_k$,

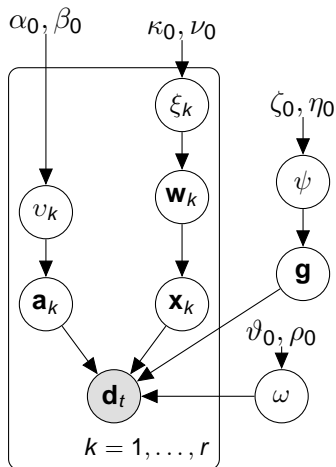$$w_{i,k} = \begin{cases} h_k & s_k \leq i \leq s_k + l_k \\ 0 & \text{otherwise} \end{cases} \tag{13}$$

Deconvolution in BSS (BCMS)

- Each time-activity curve, $\mathbf{x}_k$, is modeled as a convolution:

$$x_{t,k} = \sum_{m=1}^{t} b_{t-m+1} u_{m,k} \tag{12}$$

- Convolution kernels of each tissue are modeled as additions stored in vectors $\mathbf{w}_k$,

$$w_{i,k} = \begin{cases} h_k & s_k \le i \le s_k + l_k \\ 0 & \text{otherwise} \end{cases} \tag{13}$$

Convolution kernel u_f Differences of u_f, w_f
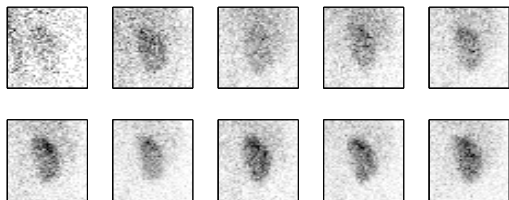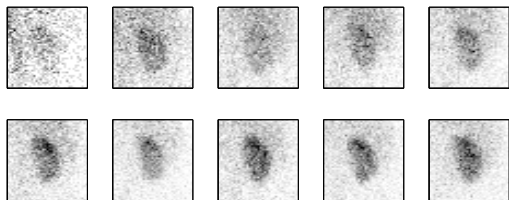
Deconvolution in BSS (BCMS)
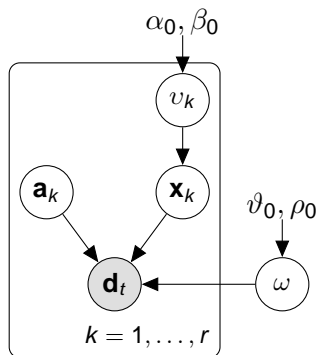
BSS+ model
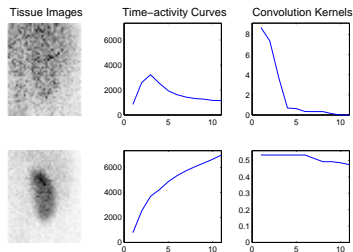
BCMS model

Deconvolution in BSS (BCMS)

Deconvolution in BSS (BCMS)

BSS+ results
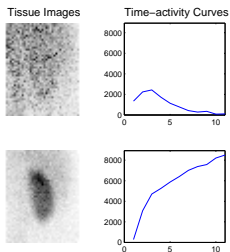
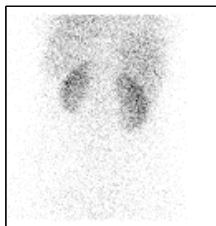BCMS results

Tissue Images — Time–activity Curves

Tissue Images — Time–activity Curves — Convolution Kernels

Automatic regions of interest in BSS (FAROI)

region
of interest

(for the right
kidney)

Automatic regions of interest in BSS (FAROI)

region
of interest
⟶
(for the right
kidney)
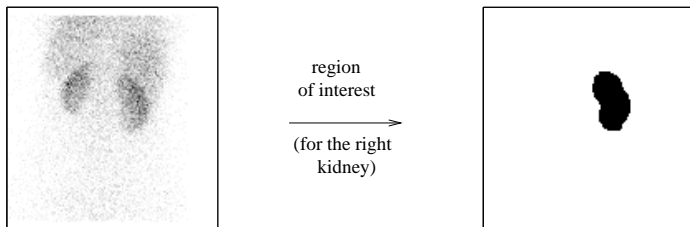
Each pixel $a_{i,k}$ in the tissue image $\mathbf{a}_k$ has an indicator variable $\mathbf{i}_{i,k}$ such that

$$\mathbf{i}_{i,k} = \begin{cases} 1 & \text{i-th pixel has non-zero activity in the k-th factor,} \\ 0 & \text{i-th pixel has zero activity in the k-th factor.} \end{cases}$$

(14)

Automatic regions of interest in BSS (FAROI)

- We would like to have two extremes:

$$f(a_{i,k}) = \begin{cases} \mathsf{U}(0,1) & \mathbf{i}_{i,k} = 1, \\ \mathsf{t}\mathcal{N}(0, \xi_k^{-1}) & \mathbf{i}_{i,k} = 0, \end{cases}$$

- $\mathsf{U}(0,1)$ is a prior model of the tissue.
- $\mathsf{t}\mathcal{N}(0, \xi_k^{-1})$ is a model of a "soft zero".

Automatic regions of interest in BSS (FAROI)

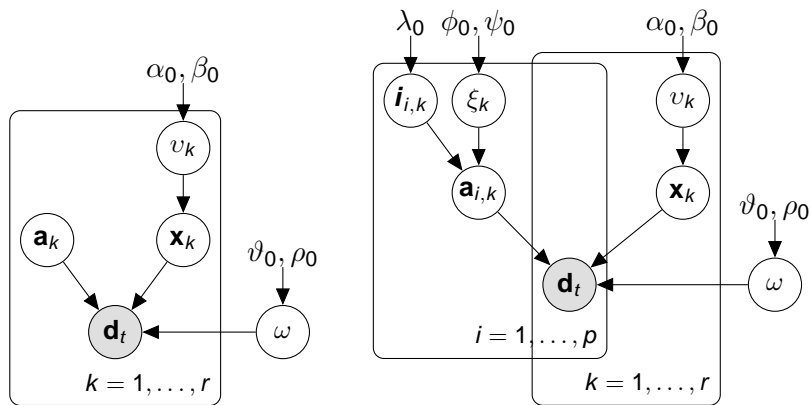- ▶ We would like to have two extremes:

$$f(a_{i,k}) = \begin{cases} \mathrm{U}(0,1) & \mathbf{i}_{i,k} = 1, \\ \mathrm{t}\mathcal{N}(0, \xi_k^{-1}) & \mathbf{i}_{i,k} = 0, \end{cases}$$

- ▶ $\mathrm{U}(0,1)$ is a prior model of the tissue.
- ▶ $\mathrm{t}\mathcal{N}(0, \xi_k^{-1})$ is a model of a "soft zero".
- ▶ We model $\mathbf{i}_{i,k}$ as a continuous variable, $\mathbf{i}_{i,k} \in \langle 0, 1 \rangle$

$$f(a_{i,k}) = \mathrm{U}(0,1)^{\mathbf{i}_{i,k}} \times \mathrm{t}\mathcal{N}(0, \xi_k^{-1})^{(1-\mathbf{i}_{i,k})} \tag{15}$$

(for computation reason)

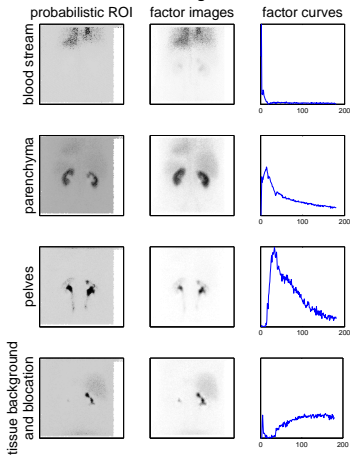# Automatic regions of interest in BSS (FAROI)
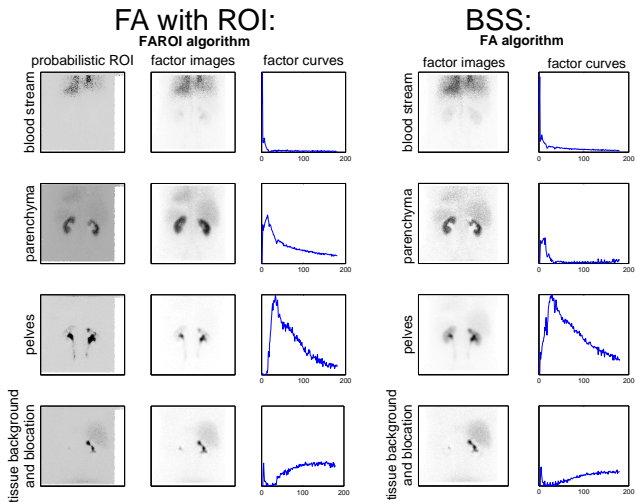
Automatic regions of interest in BSS (FAROI)

FA with ROI: BSS:

Automatic regions of interest in BSS (FAROI)

FA with ROI:
FAROI algorithm

BSS:
FA algorithm

Sparsity and deconvolution in BSS (S-BSS-vecDC)

[C.M. Bishop and M.E. Tipping. The 16th Conference on Uncertainty in Artificial Intelligence, pages 46–53, 2000.]

Automatic relevance determination (ARD) principle:

$$f(\mathbf{s}|\boldsymbol{\theta}) = \mathcal{N}(\mathbf{0}, \text{diag}(\boldsymbol{\theta})), \tag{16}$$

$$f(\theta_t) = \mathsf{G}(\alpha_0, \beta_0), \tag{17}$$

Sparsity and deconvolution in BSS (S-BSS-vecDC)

[C.M. Bishop and M.E. Tipping. The 16th Conference on Uncertainty in Artificial Intelligence, pages 46–53, 2000.]
Automatic relevance determination (ARD) principle:

$$f(\mathbf{s}|\boldsymbol{\theta}) = \mathcal{N}(\mathbf{0}, \text{diag}(\boldsymbol{\theta})), \qquad (16)$$
$$f(\theta_t) = \mathsf{G}(\alpha_0, \beta_0), \qquad (17)$$

▶ The expected value of the prior variance of a redundant parameter approaches zero in the Variational Bayes solution.

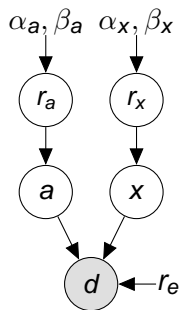# Sparsity and deconvolution in BSS (S-BSS-vecDC)

Scalar example again:
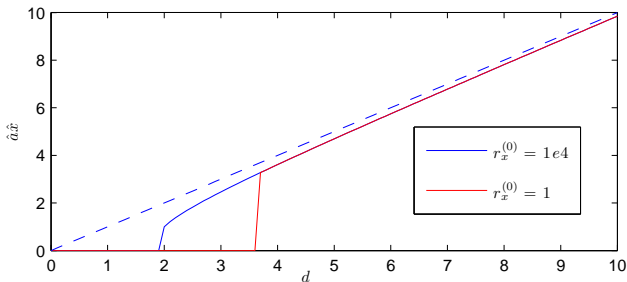
$$d = ax + e, \ e \sim \mathcal{N}(0, r_e) \tag{18}$$

Sparsity and deconvolution in BSS (S-BSS-vecDC)

Scalar example again:

$$d = ax + e, \ e \sim \mathcal{N}(0, r_e) \tag{18}$$

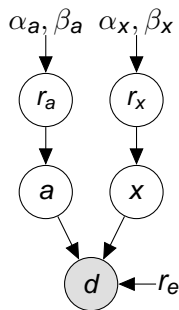$$p(a|r_a) = t\mathcal{N}(0, r_a^{-1}), \ p(\omega_a) = G(\alpha_a, \beta_a), \tag{19}$$

Sparsity and deconvolution in BSS (S-BSS-vecDC)

Scalar example again:

$$d = ax + e, \ e \sim \mathcal{N}(0, r_e) \tag{18}$$

$$p(a|r_a) = t\mathcal{N}(0, r_a^{-1}), \ p(\omega_a) = G(\alpha_a, \beta_a), \tag{19}$$

Sparsity and deconvolution in BSS (S-BSS-vecDC)

Matrix formulation of the data model:

$$D = [\mathbf{a}_1, \ldots, \mathbf{a}_r][\mathbf{x}_1, \ldots, \mathbf{x}_r]' = AX'. \qquad (20)$$

Sparsity and deconvolution in BSS (S-BSS-vecDC)

Matrix formulation of the data model:

$$D = [\mathbf{a}_1, \ldots, \mathbf{a}_r][\mathbf{x}_1, \ldots, \mathbf{x}_r]' = AX'. \tag{20}$$

▶ Each time-activity curve arrise as convolution of the input function and tissue-specific kernels as

$$\mathbf{x}_k = \mathbf{b} * \mathbf{u}_k, \ \forall k = 1, \ldots, r. \tag{21}$$

Sparsity and deconvolution in BSS (S-BSS-vecDC)

Matrix formulation of the data model:

$$D = [\mathbf{a}_1, \ldots, \mathbf{a}_r][\mathbf{x}_1, \ldots, \mathbf{x}_r]' = AX'. \tag{20}$$

▶ Each time-activity curve arrise as convolution of the input function and tissue-specific kernels as

$$\mathbf{x}_k = \mathbf{b} * \mathbf{u}_k, \ \ \forall k = 1, \ldots, r. \tag{21}$$

Thus,

$$D = AX' = A[\mathbf{u}_1, \ldots, \mathbf{u}_r]' \begin{pmatrix} b_1 & 0 & 0 & 0 \\ b_2 & b_1 & 0 & 0 \\ \ldots & b_2 & b_1 & 0 \\ b_n & \ldots & b_2 & b_1 \end{pmatrix}' = AU'B'. \tag{22}$$

▶ We adopt ARD principle for modeling A and U.

Sparsity and deconvolution in BSS (S-BSS-vecDC)

- We adopt ARD principle for modeling A and U.
- Model of pixels:

$$f(\overline{\mathbf{a}}_i|\boldsymbol{\xi}_i) = t\mathcal{N}(\mathbf{0}_{1,r}, \text{diag}(\boldsymbol{\xi}_i)^{-1}), \ \ \forall i = 1, \ldots, p, \quad (23)$$

$$f(\boldsymbol{\xi}_i) = \prod_{k=1}^{r} \mathsf{G}(\phi_{ik,0}, \psi_{ik,0}), \quad (24)$$

Sparsity and deconvolution in BSS (S-BSS-vecDC)

- Model of convolution kernels:

$$f(\text{vec}(U)|\Upsilon) = t\mathcal{N}(\mathbf{0}_{nr,1}, \Upsilon^{-1}), \tag{25}$$

$$f(\Upsilon) = \prod_{j=1}^{nr} G(\alpha_{j,0}, \beta_{j,0}), \tag{26}$$

- Vectorized form of U allows us to model the relation between convolution kernels mutually

Sparsity and deconvolution in BSS (S-BSS-vecDC)

▶ Model of convolution kernels:

$$f(\text{vec}(U)|\Upsilon) = t\mathcal{N}(\mathbf{0}_{nr,1}, \Upsilon^{-1}), \tag{25}$$

$$f(\Upsilon) = \prod_{j=1}^{nr} \mathsf{G}(\alpha_{j,0}, \beta_{j,0}), \tag{26}$$

▶ Vectorized form of U allows us to model the relation between convolution kernels mutually

▶ Model of the input function:

$$f(\mathbf{b}|\varsigma) = t\mathcal{N}(\mathbf{0}_{n,1}, \varsigma^{-1}I_n), \tag{27}$$

$$f(\varsigma) = \mathsf{G}(\zeta_0, \eta_0), \tag{28}$$

Sparsity and deconvolution in BSS (S-BSS-vecDC)
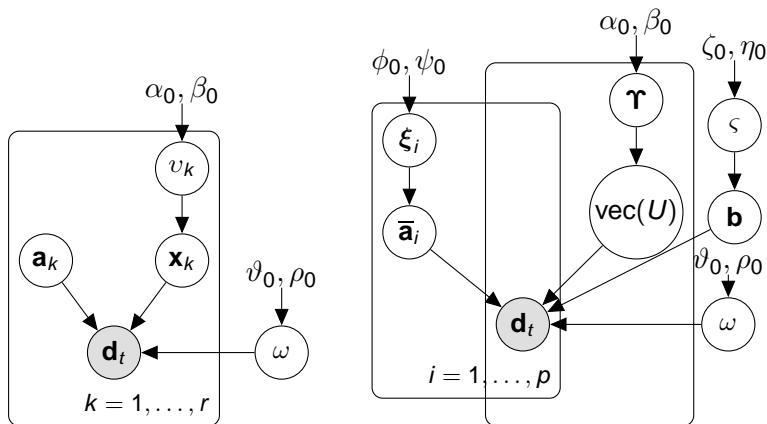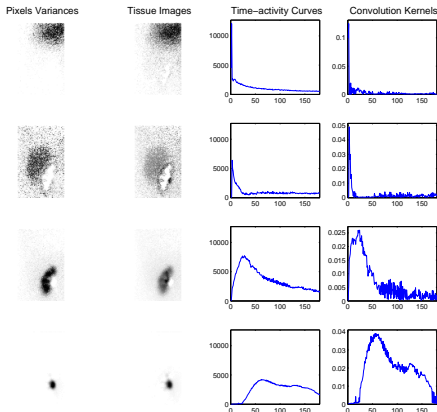
Sparsity and deconvolution in BSS (S-BSS-vecDC)

Example result:

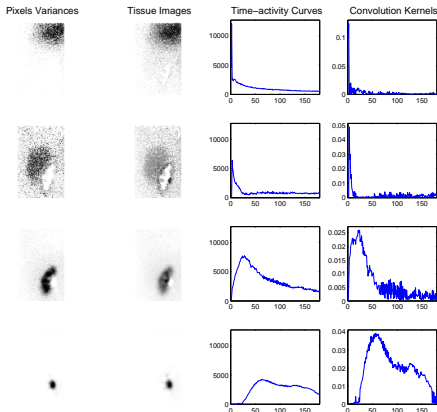S-BSS-vecDC: BSS:

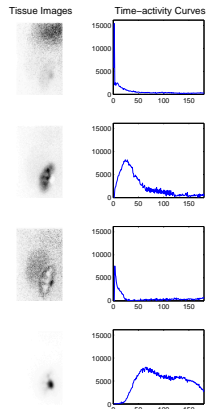# Sparsity and deconvolution in BSS (S-BSS-vecDC)

Example result:

S-BSS-vecDC: BSS:

Validation

- How to validate or compare the algorithms since typically no ground truth is available?

Validation

- ► How to validate or compare the algorithms since typically no ground truth is available?

What we can do:

- ► Validation on synthetic data.
- ► Comparison with physician's separation results.
- ► Comparison on parameters such as RRF.

Validation on Synthetic Data

We generate data composed of 3 sources and noise.
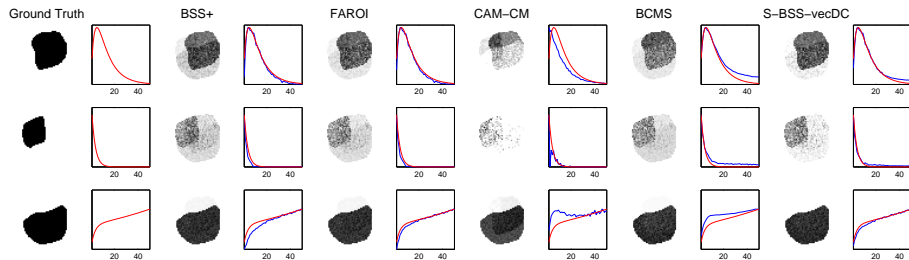
Validation on Real Data from Renal Scintigraphy

- We have 19 sequences where activities of parenchyma and heart are selected using experienced physician.

Validation on Real Data from Renal Scintigraphy

- ▶ We have 19 sequences where activities of parenchyma and heart are selected using experienced physician.
- ▶ We use these physician's results as our ground truth.
- ▶ The statistics such as MSE, MAE, or median can be calculated for the whole dataset and compared.
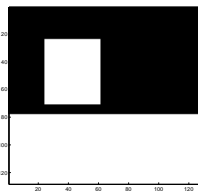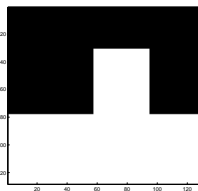
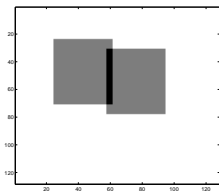# Validation on Real Data from Renal Scintigraphy

Experiment description:

- Each image has resolution 128×128 pixels.
- Each sequence contains $100 - 180$ images.

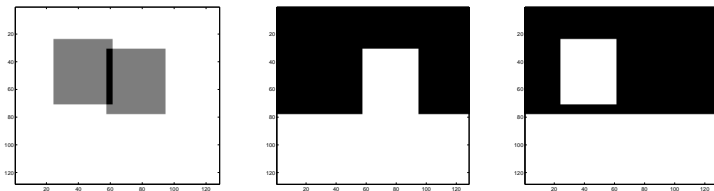# Validation on Real Data from Renal Scintigraphy

Experiment description:

- Each image has resolution 128×128 pixels.
- Each sequence contains $100 - 180$ images.
- We use automated ROIs based on those from physician hiding left or right kidney = we have 38 kidneys in experiment.

Validation on Real Data from Renal Scintigraphy

Experiment description:

- Each image has resolution 128×128 pixels.
- Each sequence contains $100 - 180$ images.
- We use automated ROIs based on those from physician hiding left or right kidney = we have 38 kidneys in experiment.
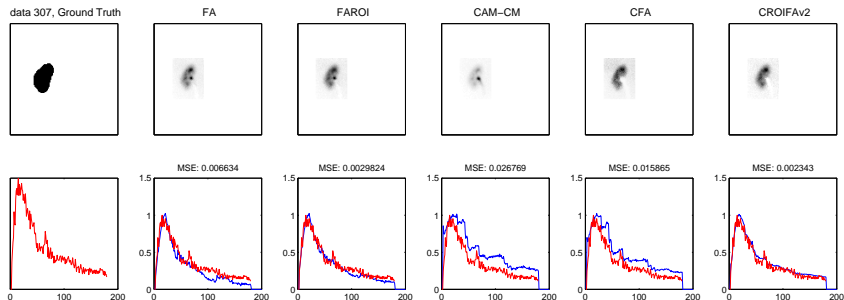

- Activity of parenchyma is examined using algorithms: BSS, FAROI, CAM-CM, BCMS, S-BSS-vecDC.

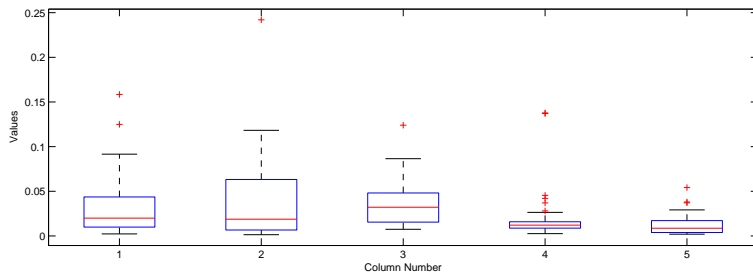# Validation on Real Data from Renal Scintigraphy

Example result:

Validation on Real Data from Renal Scintigraphy

Example result:

Validation on Real Data from Renal Scintigraphy

algorithm	mean MLE $\pm$ std MLE	mean MAE $\pm$ std MAE	best MLE	best MAE
BSS+	0.0314$\pm$0.0340	0.1197$\pm$0.0687	3	4
FAROI	0.0358$\pm$0.0469	0.1202$\pm$0.0860	9	7
CAM-CM	0.0376$\pm$0.0262	0.1444$\pm$0.0567	0	1
BCMS	0.0207$\pm$0.0296	0.0914$\pm$0.0601	10	11
S-BSS-vecDC	**0.0124$\pm$0.0118**	**0.0730$\pm$0.0376**	**16**	**15**

Validation on Real Data from Renal Scintigraphy

algorithm	mean MLE $\pm$ std MLE	mean MAE $\pm$ std MAE	best MLE	best MAE
BSS+	0.0314±0.0340	0.1197±0.0687	3	4
FAROI	0.0358±0.0469	0.1202±0.0860	9	7
CAM-CM	0.0376±0.0262	0.1444±0.0567	0	1
BCMS	0.0207±0.0296	0.0914±0.0601	10	11
S-BSS-vecDC	**0.0124±0.0118**	**0.0730±0.0376**	**16**	**15**

Clinical Validation

- 107 data sets are available on
  http://www.dynamicrenalstudy.org/ since March 2012.

Clinical Validation

- 107 data sets are available on http://www.dynamicrenalstudy.org/ since March 2012.
- Data are well described and RRFs are given.
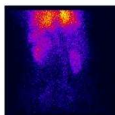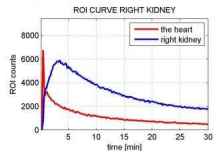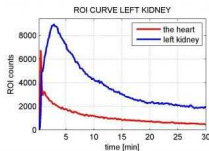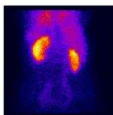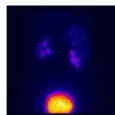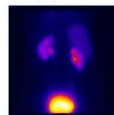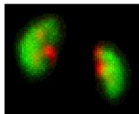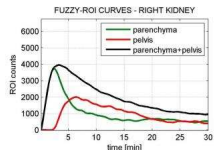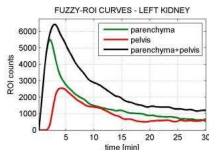
Clinical Validation

- 99 datasets are used (2 kidneys are required).

Clinical Validation

- 99 datasets are used (2 kidneys are required).
- Each dataset: 180 images taken after each 10 seconds as a matrix of 128×128 pixels.
- Part of accumulation of each sequence is selected.

Clinical Validation

- 99 datasets are used (2 kidneys are required).
- Each dataset: 180 images taken after each 10 seconds as a matrix of 128×128 pixels.
- Part of accumulation of each sequence is selected.

Our objection:

- Assessment of relative renal function using: BSS, FAROI, CAM-CM, BCMS, S-BSS-vecDC.
- Comparison with expert RRFs via cumulative histogram.

Clinical Validation

- Quantiles of the difference of the estimated RRF from the reference value for all 99 patients.

algorithm	$\leq$3%	$\leq$5%	$\leq$10%	$\geq$10%
BSS+	38.4%	57.6%	78.8%	21.2%
FAROI	43.4%	58.6%	83.8%	16.2%
CAM-CM	30.3%	48.5%	63.6%	36.4%
CFA	42.4%	59.6%	82.8%	17.2%
S-BSS-vecDC	**46.5%**	**68.7%**	**86.9%**	**13.1%**

Conclusion

- ▶ Blind source separation methods were introduced.
- ▶ Sparsity modeling of tissue images was proposed.
- ▶ Convolution model within blind source separation was proposed.
- ▶ Comparison on both synthetic and real data was given.

Thank you for your attention.
Questions?